Macromolecules

pubs.acs.org/Macromolecules Article

Fabrication of Elastic Copolyester by Incorporation of Aliphatic Long-Chain in Poly(1,4-Cyclohexylenedimethylene furanoate)

Yajin Fang, Tao Yang, Fei Liu,* Jinggang Wang,* and Jin Zhu

Cite This: *Macromolecules* 2025, 58, 8833−8844 Read Online

ACCESS | Metrics & More | Article Recommendations | Supporting Information

ABSTRACT: The widespread use of petroleum-based plastics has resulted in significant environmental and health issues, highlighting the urgent need for biobased high-performance polymers to foster a sustainable future. Biobased elastomeric materials are particularly advancing to improve the performance of biobased polymers. This study seeks to develop environmentally friendly elastomers with properties comparable to those of petroleum-based olefin elastomers while maintaining the advantages of thermoplastic polyesters. Herein, the biobased dodecanedioic acid was introduced to the biobased polyester composed of 2,5-furandicarboxylic acid and 1,4-cyclohexanedimethanol, in order to construct poly(1,4-cyclohexylenedimethylene dodecanedioate-co-furanoate) (PCDF) copolyester with tunable mechanical properties. Notably, PCDF copolyester containing 60% of aliphatic long-chain in its diacid content exhibits an elastic modulus of 52 MPa and an impressive recovery rate of 64% to its original state after stretching to 200% strain. Different from the traditional strategy of using a polyether soft segment to realize elasticity, this study proposed an interesting and simple strategy to fabricate a biobased copolyester with an elastic property by merely using a biobased aliphatic long-chain.

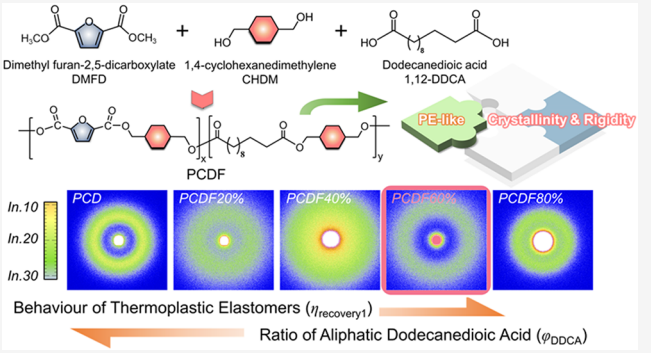

1. INTRODUCTION

Elastomers have been extensively used in diverse industrial sectors and have attracted more and more attention in emerging fields such as regenerative medicine, soft robotics, and stretchable electronics.[1,2] Nevertheless, within the family of elastomers, thermoplastic polyester elastomers (TPEs) are widely recognized as the most promising alternative to high-performance engineering materials due to their excellent mechanical strength and toughness, and play important roles in manufacturing, engineering, medical, and military fields due to their excellent properties.[1,3−6] Due to the overconsumption of fossil resources and the global push for carbon peaking and neutrality, the use of renewable monomers and green polymerization processes for the synthesis of TPEs is increasingly relevant.[7−9]

Biobased elastomers can enhance sustainability when derived from renewable monomers, with 2,5-furandicarboxylic acid (FDCA) emerging as a promising candidate.[10,11] The asymmetrical structure of FDCA creates an efficient spiral motif for performance release, while its ring structure contributes to the hard elastomer domain.[12,13,13] In multiblock copolymers, renewable FDCA can be used as a source of rigidity for crystallizable hard-segmented structures, significantly enhancing the mechanical strength of TPEs.[14−21] Among them, FDCA-derived poly(neopentyl glycol 2,5-furandicarboxylate) (PNF) and poly(1,4-cyclohexanedimethylene furandicarboxylate) (PCF) are two examples for the development of biobased TPEs with high performance.[19,20,22−24] Despite several decades of research and development in TPEs, traditional synthesis strategies have typically focused on incorporating amorphous and flexible polyether soft segments into thermoplastic polymer chains.[2,4] The above-mentioned advances for the development of biobased TPEs with biobased aromatic monomers still followed the same strategies.[19,20,22−25] Normally, TPEs, consisting of hard end blocks A (a semicrystalline thermoplastic with a T_m > room temperature or an amorphous thermoplastic with a T_g > room temperature) and a soft midblock B (a soft, rubbery, and flexible amorphous polymer with a T_g < room temperature), show potential as eco-friendly substitutes for nonrenewable. Nevertheless, few studies have been reported on the design of TPEs without the use of conventional amorphous soft segments. Therefore, it is interesting to develop an alternative methodology to synthesize TPEs without using a polyether soft segment.[26−29]

Received: April 25, 2025
Revised: July 28, 2025
Accepted: August 5, 2025
Published: August 9, 2025

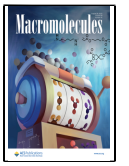

Downloaded via ECOLE POLYTECHNIC FED LAUSANNE on October 28, 2025 at 14:27:30 (UTC).
See https://pubs.acs.org/sharingguidelines for options on how to legitimately share published articles.

ACS Publications © 2025 American Chemical Society

https://doi.org/10.1021/acs.macromol.5c01114
Macromolecules 2025, 58, 8833−8844

Scheme 1. Schematic Illustration for the Synthesis of PCDF Copolyesters

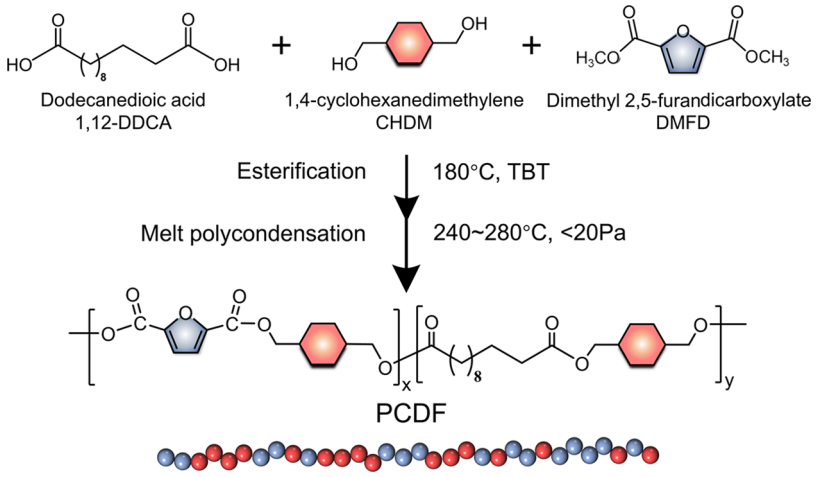

Aliphatic polyesters with long methylene repeat units are excellent elongable mechanical materials that are used in a broad range of uses such as food packaging that has similar properties to high density polyethylene (HDPE), depending on its molecular weight and can be enzymatically degraded.[30−32] Initially, long-chain ω-hydroxy fatty acids, suitable as AB-monomers for polyesterification, were generated by Gross et al. with engineered yeast strains.[33] A number of interesting materials have been obtained by melt polycondensation with short-chain diols.[34,35] According to Zhou et al., PE-2,11 essentially translates to the crystalline structure being dominated by the hydrocarbon chains' order and arrangement, as in typical HDPE folded-chain crystallites.[36] Goto et al. synthesized a series of biomass-based linear aliphatic polyesters by combining sebacic acid and 1,18-octadecanedioic acid with various diols of differing alkyl chain lengths. These polyesters exhibited relatively high T_m values ranging from 78 to 93 °C, comparable to those of low-density polyethylene (LDPE), which has T_m values between 105 and 118 °C. Consequently, these biomass-based polyesters can serve as a thermal alternative to LDPE regarding thermal performance and mechanical properties. Recently, by incorporating 1,12-dodecanedioic acid (DDCA) into the traditional petroleum-based poly(butylene terephthalate)-poly(tetramethylene glycol), we were able to obtain partially substituted TPE with enhanced properties.[36] DDCA modifies the microphase separation between the soft and hard segments by forming a crystallizable polyethylene-like structure with short-chain diols, which enables the modulation of properties.[36] Moreover, with the addition of only 10% of DDCA to the poly(propylene 2,5-thiophenedicarboxylate), the resulting copolyester showed significantly increased elongation at break from 3 to 735%, and displayed interesting elastic properties.[37]

Inspired by these studies, we propose to use DDCA as a comonomer for the fabrication of biobased TPEs without using a polyether soft segment. Herein, we report the design and synthesis of a series of FDCA-based copolyesters by the incorporation of DDCA as a comonomer. The effects of DDCA on the molecular structure, thermal and mechanical properties, and elastic properties were systematically investigated. This study provides a new structural design approach for developing novel biobased TPEs, thus positioning these FDCA-based copolyesters as ideal alternative materials for TPE systems, offering both stiffness and high elasticity.

2. EXPERIMENT SECTION

2.1. Materials. 1,12-Dodecanedioic acid (DDCA, 99%), tetrabutyl titanate (TBT, ≥ 99.0%), and 1,4-cyclohexanedimethanol (CHDM, 99%, *trans*/*cis* = 68/32) were purchased from Aladdin Reagent Co., Ltd. (Shanghai, China). Dimethyl 2,5-furandicarboxylate (DMFD, 99%) was supplied by Chem Target Technologies Co., Ltd. (China), and HPLC-grade chloroform and deuterated trifluoroacetic acid (TFA-d, 99.5%) were bought from Sinopharm Chemical Reagent Co., Ltd. (Shanghai, China).

2.2. Polymer Design and Preparation. PCDF copolyesters were synthesized by transesterification and melt polycondensation at a fixed total stoichiometry of raw materials; by controlling the feed ratio of the raw materials in the stages of transesterification, it is possible to manipulate the sequence length. In the first step, carried out at 180 °C, oligomers with $COOCH_3$ and CH_2OH end groups were obtained. After that, the reactor was connected to a vacuum pump and the temperature was maintained at 180 °C or increased to 200−280 °C depending on copolyester composition. This allowed the release of methanol byproduct, obtaining high molecular weight polyesters. As shown by Scheme 1, PCDF copolyesters were synthesized by a two-step procedure using DMFD, DDCA, and CHDM. Detailed reaction conditions were summarized in Table S1 for the different compositions of copolyesters. The synthesized compounds were dubbed PCDF*x*%, where "*x*" denoted the content of the DDCA from 20 to 80 mol % (Scheme 1). For comparison, the PCD homopolyester was prepared under similar conditions. Every sample was analyzed without further purification.

2.3. Characterization Methods. The structural and compositional characteristics of PCDF copolyesters were systematically investigated using proton and carbon nuclear magnetic resonance (^{1}H- and ^{13}C NMR) spectroscopy on a Bruker AVANCE NEO 600 NMR spectrometer operating at 600 MHz at ambient temperature, utilizing $CDCl_3$ as the solvent. The intrinsic viscosities ($[\eta]$) of the PCDF copolyesters were determined with a capillary Ubbelohde viscometer at 25 °C in a 50/50 wt % phenol-tetrachloroethane solution (Aladdin, AR). Attenuated total reflectance (ATR) Fourier transform infrared (FT-IR) spectroscopy was performed at room temperature, employing an Agilent Cary 660 + 620 FT-IR micro spectrometer.

https://doi.org/10.1021/acs.macromol.5c01114
Macromolecules 2025, 58, 8833−8844

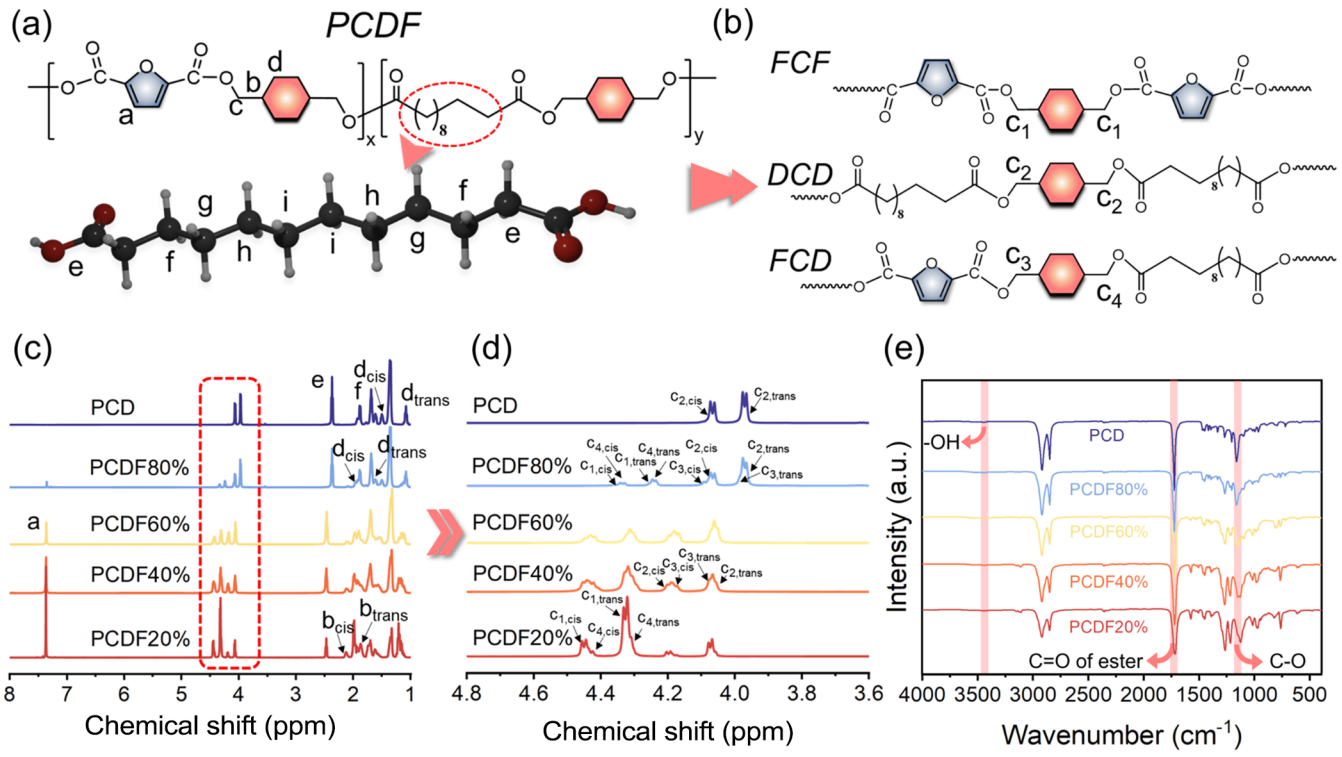

Figure 1. (a) Chemical structure, (b) sequence structure of triads in PCD and PCDF copolyesters, (c) ^{1}H NMR, and (d) spectra of sequence structure of triads. (e) FT-IR spectra of PCDF copolyesters and PCD.

To ascertain the number-average molecular weight (M_n), weight-average molecular weight (M_w), and molecular weight distribution ($Đ$) of the samples, gel permeation chromatography (GPC) was conducted at 40 °C, utilizing HPLC-grade chloroform as the eluent on an Agilent PL-GPC220 system. The crystallinity of the final products was analyzed via X-ray diffraction (XRD) with a Bruker D8 Advance Davinci diffractometer, scanning over a 5 to 50° angle range at a rate of 2°/min.

Thermal properties of the PCDF copolyester samples were characterized using differential scanning calorimetry (DSC, Mettler-Toledo DSC III) across a temperature range of −70 to 280 °C, with heating and cooling rates set to 10 °C/min. The thermal stability was assessed through thermogravimetric analysis (TGA) using a Mettler-Toledo TGA/DSC apparatus in a ceramic furnace, applying a heating rate of 10 °C/min from 50 to 800 °C under nitrogen and air atmospheres.

Dynamic mechanical properties of the annealed PCDF copolyester samples were evaluated using a dynamic mechanical analyzer (DMA Q850, TA Instruments) at a frequency of 1 Hz, employing a multifrequency strain mode across a temperature range of −100 °C to just below the melting temperature (T_m), with a heating rate of 3 °C/min.

Small-angle X-ray scattering (SAXS) measurements were conducted by using a Xeuss 3.0 instrument (Xenocs), featuring a Cu target and a Pilatus 300 K detector, with the detector positioned 800 mm from the sample. All data were corrected for air and background scattering at RT. A one-dimensional correlation function $K(z)$, as defined by Strobl and Schneider,[39−41] was employed to evaluate the average values of the long period (L), lamellar thickness (L_c), and amorphous size (L_a).

The key mechanical properties of the PCDF copolyesters were assessed at room temperature using an Instron 5567 tensile testing machine (Zwick/Roell Z1.0) equipped with a 1 kN load cell. Extension rates were maintained at 100 mm/min during the tensile tests to ensure consistent measurement conditions.

For additional details regarding sample handling, experimental methodologies, and characterization procedures, please refer to the Supporting Information section. This comprehensive approach to characterization enables a thorough understanding of the structural, thermal, and mechanical properties of PCDF copolyesters, thus contributing to the development of high-performance materials for relevant applications.

3. RESULTS AND DISCUSSION

3.1. Fabrication and Characterization of PCD and PCDF Copolyesters. The synthetic routes of the PCDF copolyesters are listed in Scheme 1. Five samples were obtained: PCDF20%, PCDF40%, PCDF60%, PCDF80%, and PCD. The molecular structure (Figure 1a,b) and structural information (Figure 1c,d) of the obtained copolyesters are shown in Figure 1. The ^{1}H NMR (Figure 1c,d) spectra showed that the synthesized product agreed with the targeted PCF and PCD, and the expected characteristic peaks with matching chemical shifts for the repeating segments derived from FDCA, DDCA, and CHDM are observed. Briefly, melt transesterification utilizing TBT as a catalyst and conventional melt polycondensation produced (co)polyesters with varying CHDM isomer incorporation. By evaluating the area of corresponding characteristic peaks (eq S1, S2), the relative mole ratios of CF and CD segments in PCDF are calculated, indicating high conformity with the initial feeding, as summarized in Table S1 (Supporting Information).

The ^{1}H NMR spectra were displayed to verify the chemical structure of the synthesized copolyesters. The spectra of both

https://doi.org/10.1021/acs.macromol.5c01114
Macromolecules 2025, 58, 8833−8844

Table 1. Structures and Molecular Weight of PCD and PCDF Copolyesters

specimens	L_{PCD}	L_{PCF}	R	M_n[a] (g/mol)	M_w[a] (g/mol)	$Đ$[a]	φ_{CD}[b]	$[\eta]$ (dL/g)
PCDF20%	4.21	1.43	0.94	35,600	61,200	1.72	19.6	1.11
PCDF40%	6.20	1.30	0.94	32,300	57,800	1.79	39.9	1.06
PCDF60%	8.92	1.23	0.93	37,200	70,700	1.90	59.8	1.12
PCDF80%	14.19	1.13	0.96	45,600	85,700	1.87	80.1	1.08
PCD	-	-	-	42,400	83,900	1.98	100	0.82

[a]Molecular weight dispersity from GPC.

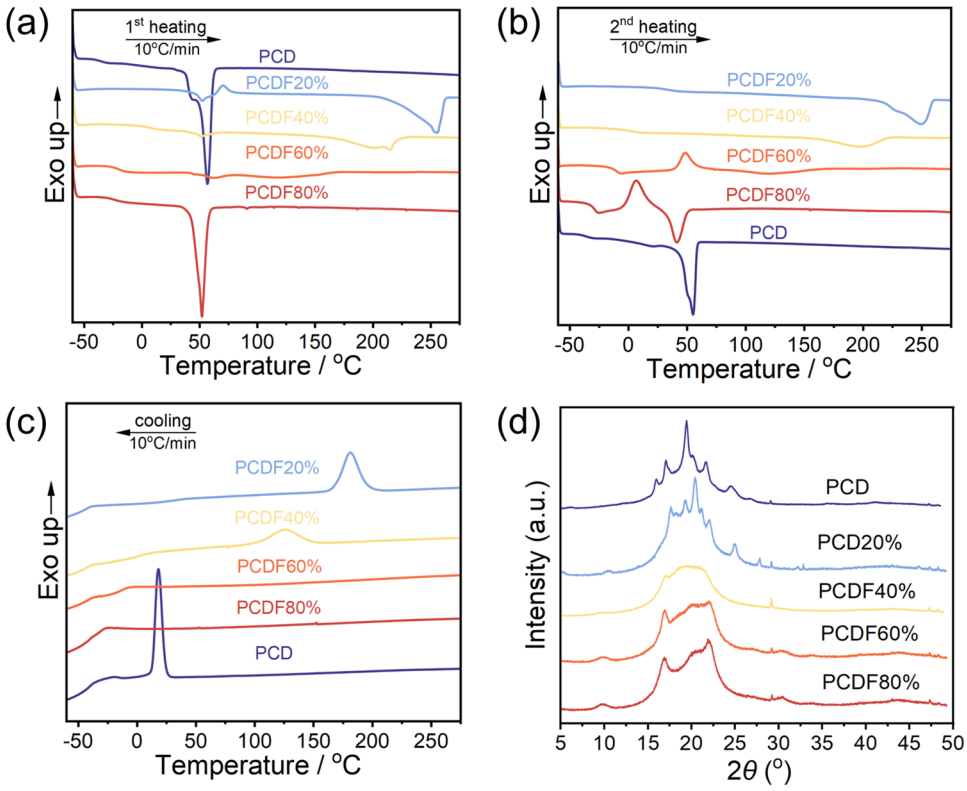

Figure 2. DSC curves of PCD and PCDF copolyesters in (a) the first heating scans, (b) the second heating scans, and (c) cooling scans. (d) XRD patterns for PCD and PCDF copolyesters.

PCD and PCDF copolyesters exhibit two main peaks at 7.22 (I_a) and 4.65 (I_b) ppm (see Figure 1c) assigned to the furan ring ($-C_4H_2O-$) and methylene of CHDM, respectively. The copolyester compositions were determined by spectra, using the signals corresponding to the CH2CO of both the furan ring and PCD units, which appeared at 2.61 and 2.28 ppm, respectively. In ^{1}H NMR, the signals showing at 2.52, 1.73, and 1.40 ppm were assigned to $-CH_2-$ in the DDCA segments (proton f–i), while that at 4.17 (c_{trans}) ppm and 4.29 ppm (c_{cis}) to the methylene groups connected with ester bonds at *trans*- and *cis*-form of cyclohexanedimethylene repeating units, respectively.[20,37,42−44]

Consequently, the compositional ratio of each copolyester was calculated by integrating appropriate ^{1}H NMR peaks to verify that the compositional ratio matches the feed ratio, and when compared to the theoretical value, the difference is just 0.4%.[42,45] There were three kinds of possible chain structures in these copolyesters (Figure 1b). Once the high chemical-shift region of ^{1}H NMR is magnified in the enlarged image (Figure 1d), four new proton peaks can be observed at 4.5 (c_1), 4.3 (c_2), 4.2 (c_3), and 4.1 (c_4) ppm for all PCDF copolyesters.

$$\varphi_{CD} = \frac{I_e}{I_e + 2I_a} \times 100\% \quad (1)$$

where characteristic peaks involving molecular weights were 356 (CD segment unit) and 282 (CF segment unit), respectively. Figure 1 displays the three repeating units of FCD, DCD, and FCF in PCDF copolyesters together with the matching unique peaks in ^{1}H NMR spectra. FCD, DCD, and FCF reflect three sequence configurations of CHDM connected to DDCA or FDCA on both sides, as indicated by characteristic peaks c_1, c_2, c_3, and c_4. Using ^{1}H NMR spectra and eqs (S3−S5), the average sequence length of PCD (L_{PCD}), PCF (L_{PCF}), and degree of randomness (R) were determined. Table 1 shows that, while the φ_{CD} increases, the L_{PCD} values of the CD segment increase significantly from 4.21 to 14.19, while the L_{PCF} values of the CF segment decrease slightly from 1.43 to 1.13. Subsequent analysis of the thermal properties will offer insights into the compatibility of two kinds of segments, as well as the alterations in the synergistic modification of the crystalline phase with two different diacids. The R in the copolyesters was determined through ^{1}H NMR analysis, yielding values of 0.93−0.96, which are close to 1. This

https://doi.org/10.1021/acs.macromol.5c01114
Macromolecules 2025, 58, 8833−8844

Table 2. Thermal Properties of PCD and PCDF Copolyesters[a]

	cooling scan		first heating scan				second heating scan				
samples	T_c (°C)	ΔH_c (J/g)	T_{cc1} (°C)	ΔH_{cc1} (J/g)	T_{m1} (°C)	ΔH_{m1} (J/g)	T_{cc2} (°C)	ΔH_{cc2} (J/g)	T_g (°C)	T_{m2} (°C)	ΔH_{m2} (J/g)
PCDF20%	181.2	38.6	70.0	3.1	255.7	42.6	n.d.	n.d.	39.4	249.5	35.6
PCDF40%	125.6	24.8	n.d.	n.d.	214.4	21.7	n.d.	n.d.	5.5	197.7	19.6
PCDF60%	n.d.	n.d.	n.d.	n.d.	121.1	8.3	48.3	12.5	−11.2	119.8	10.4
PCDF80%	n.d.	n.d.	n.d.	n.d.	57.0	44.8	41.2	17.7	−29.2	66.6	31.8
PCD	18.0	43.6	n.d.	n.d.	56.6	58.2	n.d.	n.d.	−35.4	55.1	37.7

[a]n.d. represents not detected

finding indicates the successful synthesis of a series of PCDF copolyesters with randomly distributed segments.

Figure 1e shows the FT-IR spectra of PCD and PCDF copolyesters, in which the peak at 1712 cm^{-1} displays the C═O of ester groups, and the C−H out-of-plane deformation of two carbonyl substituents on the aromatic ring depicts at 730 cm^{-1}. The two peaks at 1410 and 1240 cm^{-1} are ascribed to $-CH_2-$ deformation band and C(O)−O stretching of ester groups, respectively. The asymmetric and symmetric aliphatic C−H stretching vibrations were detected at 2907 and 2968 cm^{-1}, respectively, for PCF. However, in PCDF copolyesters, the peaks attributed to C−H stretching were shifted to the lower wavenumbers at 2852 and 2924 cm^{-1}, which is due to the presence of methyl groups in the structure of this polymer. Moreover, it was clearly visible for PCDF copolyesters, reduced in intensity as the content in PCD units increased in the copolyesters. The results from both ^1H NMR and FT-IR analyses confirm the successful synthesis of PCDF copolyesters using the selected monomers with the designed composition and functional groups. The synthesized samples have similar molecular weights (M_n) of approximately 40,000 g/mol, comparable to industrial standards. According to the results of GPC, their M_n ranged from 32,300 to 45,600 g/mol, with polydispersity between 1.72 and 1.90, and intrinsic viscosity between 1.06 and 1.12 dL/g. (Figure S1 and Table 1).

3.2. Thermal Properties. DSC and XRD analyses were used to examine the thermal characteristics of PCDF copolyesters. The polymers were all semicrystalline with phase-separated microstructures, as determined by DSC. Figure 2(a, b) depicts the DSC curves of PCDF copolyesters in the first and second heating, respectively. Table 2 summarizes the results. It is noted that when the DDCA took the place of the FDCA, the rigidity of segments was nearly unchanged, even though there was a compliant aliphatic chain in the DDCA. Relatively low T_g of PCDF60% and PCDF80% (<−10 °C) ensured good low-temperature resistance, especially when used as soft packaging.

The first and second heating scans are shown in Figure 2a,b. The T_m of PCDF copolyesters was in a broad range of 67−250 °C; this is due to the structural differences between aliphatic and aromatic diacids. Unbranched aliphatic polyesters generally have lower T_m and T_g, yet the crystallization ability is comparable or even superior to that of aromatic polyesters, such as PBS. Indeed, furan-based copolyesters containing ≥ 80 mol % of PCD units can crystallize by forming PCD crystals. Jia et al. reported that PEDF-70, PEDF-80, and PEDF-90 had the same crystal structure as PED.[42] And the decreasing T_g was due to the increasing content of flexible PCD units in the copolyesters. When the φ_{CD} was increased further, multiple melting peaks were observed for PEDF-80, which were similar to those of the majority of polyesters. In comparison, PCDF copolyesters with 60 and 80 mol % FDCA exhibit comparable or higher T_m values than those of poly(butylene 2,5-furandicarboxylate) (PBF).[46] The crystalline mass fraction (X_c) (See Table S3) was calculated based on the measured ΔH_m from the second heating scans, the enthalpy of 100% crystalline PCF,[44,47] and the weight fraction of the CF segments (ω_{CF}). The crystallinity values for PCDF copolyesters decreased from 27.8 to 12.6% when φ_{CD} increased from 20 to 40%, suggesting that the introduction of DDCA disrupts crystallization. However, further increasing φ_{CD} to 60 and 80%, the crystallinity also increased from 20.6 to 28.3%, indicating that the crystallinity was dominated by CD segment units. Additionally, the presence of a single glass transition in the copolyesters indicates good thermodynamic compatibility between the two components, with no evidence of microphase separation occurring. In addition, during the cooling process, as illustrated in Figure 2c, samples with φ_{CD} values of 40 and 20% exhibit distinct crystallization peaks, while there is no crystallization peak for those with φ_{CD} values of 60 and 80%.

The XRD analysis (Figure 2d) demonstrates that the crystal structure and melting behavior of the copolymers are strongly influenced by the incorporation of DDCA. As φ_{CD} increases, the diffraction peaks associated with the CF segments gradually weaken, while new reflections at 21.4, 23.8, and 26.2° corresponding to the (110), (200), and (210) planes of the monoclinic α-crystal form of PCD, respectively, emerge. This structural evolution aligns with the DSC results, where the T_m shifts from 249.5 °C (CF-rich copolyesters) to 55.1 °C (PCD homopolyester), confirming that DDCA disrupts the packing of CF-dominated crystals while promoting PE-like ordering at higher φ_{CD} contents.[31,32]

Moreover, the persistence of reflection peaks at 17.8 and 22.8° across all samples suggests a partial retention of orthorhombic crystallinity, akin to linear PE, and with reduced intensity as φ_{CD} decreases.[20,47] This observation supports the DSC-derived conclusion that incorporation of DDCA progressively suppresses long-range crystallinity, leading to broader melting endotherms with the patterns displayed in Figure 2c. The combined XRD/DSC data thus reveal a structure−property relationship governed by φ_{CD}: (1) at low φ_{CD}, CF segments dominate, maintaining high T_m and losing PE-like crystallinity; (2) at intermediate φ_{CD}, CF and DC chain segments with reciprocal inhibition of crystallization can lead to competitive crystallization, thus lowering T_m and bringing about structural disturbances; (3) at high φ_{CD}, PCD-type crystals prevail, yielding a distinct low-T_m endotherm.

Compared with the thermal stability of other polyesters, PCD demonstrated excellent thermal stability, with thermal decomposition occurring in a single major step. The temperatures for the maximum decomposition rate ($T_{d,max}$) and for 5 and 50% weight loss ($T_{d,5\%}$ and $T_{d,50\%}$) were found to be 437.8, 390.8, and 439.6 °C, respectively. TGA was employed to evaluate the thermal stability of PCDF, with

https://doi.org/10.1021/acs.macromol.5c01114
Macromolecules 2025, 58, 8833−8844

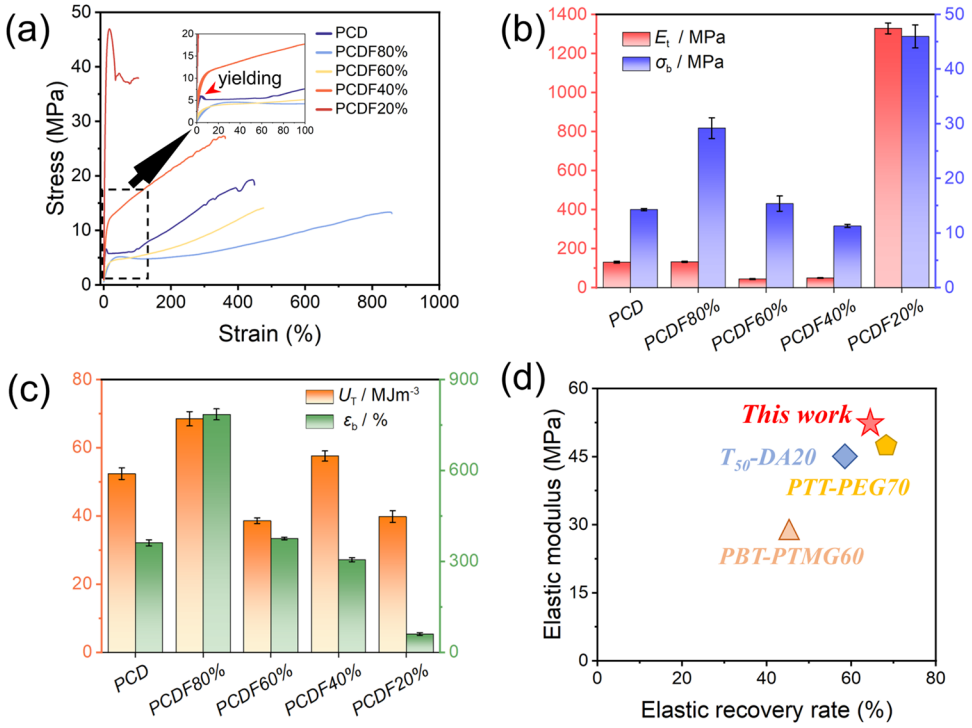

Figure 3. (a) Representative tensile strain−stress curves of PCDF copolyesters. (b) Intuitive E_t and σ_b and curves. (c) ε_b and U_T curves of PCD and PCDF copolyesters. (d) Ashby plot of stiffness (E_t) and elasticity (η_{r1}): comparing the performance of PCDF60% with conventional TPEs.

Table 3. Tensile Properties of PCD and PCDF Copolyesters

sample	E_t (MPa)	σ_y (MPa)	ε_y (%)	σ_b (MPa)	ε_b (%)	U_T (MJm^{-3})
PCDF20%	1329 ± 28	46.0 ± 2.1	21.2 ± 1.7	37.4 ± 1.8	61 ± 5	39.8 ± 3.1
PCDF40%	133 ± 2	-	-	29.2 ± 0.3	301 ± 29	57.5 ± 2.5
PCDF60%	52 ± 2	-	-	11.5 ± 1.4	377 ± 23	38.6 ± 1.8
PCDF80%	80 ± 3	5.0 ± 0.3	98.2 ± 4.3	15.1 ± 1.9	767 ± 37	68.5 ± 2.1
PCD	183 ± 5	8.2 ± 0.2	9.2 ± 1.1	14.2 ± 0.2	361 ± 13	52.4 ± 2.8

Figure S2 summarizing the weight loss and temperature profiles in nitrogen and air environments. In contrast, the pyrolysis of PCDF occurred in two distinct stages in air, closely related to the FDCA content, as illustrated in Figure S2d. Specifically, replacing FDCA with DDCA units resulted in a weak decrease in both $T_{d,5\%}$ and $T_{d,max}$, which were approximately 365 and 400 °C, respectively. TGA results indicate that PCDF remains stable up to 350 °C with no noticeable decomposition. By reprocessing this type of thermoplastic polyester through melting, its reshaping ability is maintained without any noticeable discoloration. The thermal gravimetric analysis curve showed that PCDF loses 5% of its original mass at 340 °C in air, confirming its excellent thermal stability (Figure S2 and Table S2).

3.3. Mechanical and Elastic Properties of PCDF Copolyesters. After conducting a thorough investigation into the molecular structure and thermal properties, we performed tensile experiments to evaluate the mechanical and elastic properties of the PCDF copolyesters. Figure 3a illustrates an example of tensile strain−stress curves, while Table 3 summarizes the relevant outcomes. All copolyesters exhibit a relatively typical elastic modulus, ranging from 52 to 1329 MPa. Theoretically, as the content of PCD units increases, the elastic modulus is expected to drop, as these units serve as the flexible domains in PCDF copolyesters.

The mechanical properties of PCD and PCDF copolyesters were directly compared to assess the impact of biobased DDCA in FDCA and CHDM-containing polymer systems. Notably, PCDF copolyester with 20% CD achieves a remarkable tensile strength (σ_b) of 46 MPa while maintaining an elastic modulus (E_t = 1329 MPa) nearly equivalent to that of PBF (1351 MPa), but relatively lower than that of PCF (2100 MPa), demonstrating comparable stiffness characteristics.[48,49] Conversely, the PCDF copolyester with 80% CD demonstrates the highest elongation at break (ε_b) of 767% and ultimate toughness (U_T) of 68.5 MJ/m^3. The flexibility of the polymer chains, indicated by the T_g value, and the molecular weight are critical factors influencing the mechanical response. This is likely attributed to the presence of asymmetric aromatic rings in PCDF, which disrupt the overall symmetry of the polymer and affect the linear stacking position. This disruption results in significant changes in the E_t and σ_b of PCDF60%.

Additionally, the spacing of the crystal surfaces varies with the DDCA component, revealing a flaw in the copolymers. This fault occurs at 60% DDCA, indicating that copolyesters with less than 60% DDCA maintain a PCF crystal structure that contains CD units. In contrast, copolyesters with more than 60% DDCA transition to a PCD crystal structure, which comprises CD units. Thus, at 60% DDCA, a conversion between PCD and PCF crystal types occurs, highlighting a competitive effect between the two distinct crystal structures

https://doi.org/10.1021/acs.macromol.5c01114
Macromolecules 2025, 58, 8833−8844

Table 4. Elastic Properties of PCD and PCDF Copolyesters[a]

sample	η_{r1} (%)	η_{r2} (%)	η_{r3} (%)	η_{r4} (%)	η_{r5} (%)
PCDF40%	36.8 ± 1.3	95.3 ± 0.5	97.8 ± 0.7	98.2 ± 0.4	99.1 ± 0.5
PCDF60%	64.0 ± 1.8	94.4 ± 0.6	97.3 ± 0.5	98.1 ± 0.3	98.6 ± 0.5
PCDF80%	45.2 ± 1.8	94.4 ± 0.6	97.3 ± 0.5	98.1 ± 0.3	98.6 ± 0.5
PCD	15.4 ± 1.7	91.6 ± 0.8	95.3 ± 0.2	96.7 ± 0.4	98.3 ± 0.3

[a]Shape recovery ratio at 200% strain using a cyclic tensile test demonstrates elastic property.

and finally endowing this copolyester with a distinct elastic property.

Compared to PCF,[44,47] in addition to the improved extensibility and stiffness, it is worth noting that the introduction of long-chain units constitutes a special structure for the coexistence of PE and polyester, and in particular, in PCDF60, a significant resilience property emerges. The mechanical properties of PCDF copolyesters were investigated, and in order to show the advantages of polymer elastomers without the addition of polyether soft segments, they were compared with biobased materials and widely used engineering elastomers (Figure 3d). The preparation of biobased elastomers without soft segments to achieve stiffness, elasticity, and toughness is a work of great importance in elastomer research. Cyclic tensile testing was used to examine the elastic deformability and reversibility of the samples to analyze their rubber behavior. Figure S3 shows the impressive cyclic tensile stress−strain curves for the copolyesters with the maximum strain (ε_{max}) set at 200%. Each of the samples exhibited significant hysteresis loops; however, their recovery processes varied considerably, and the formal recovery ratios (R_r) at 200% strain in five consecutive cycles are shown in Table 4. For the quantitative study of recovery, the recovery efficiency (η_r) is defined as follows

$$\eta_{r(n)} = \left(1 - \frac{\varepsilon_{residual}}{\varepsilon_{max}}\right)_n \times 100\% \quad (2)$$

TPE constructs networks with physical contacts as nodes, and these variables motivate the molecular chains to revert to their entangled states after unloading. PCDF60%, a semicrystalline TPE, contains plenty of entangled flexible chains with excellent elastic recovery, corresponding to recovery rates of 64.0, 94.4, 97.3, 98.1, and 98.6% for the five-cycle cyclic tensile test, respectively. During deformation, polymer chains tend to orient themselves along the deformation axis within a loosely cross-linked network that contains numerous entangled flexible chains. The coexistence of covalent cross-links and entanglements of long polymer chains impart good resilience to the elastomer. These entanglements function as slip-links, effectively transmitting tensile stress when the elastomer is stretched. The preparation of high modulus elastomers was achieved by PCDF60% exhibiting significant elastic modulus (52 MPa) and elasticity (η_{r1} = 64.0%). Compared with traditional TPEs, PCDF60% has a similar elastic response, but its modulus of elasticity is significantly higher than that of TPEs containing soft segments, achieving a reasonable balance between elasticity and rigidity.[37,50−54]

In addition, the incorporation of DDCA into the molecular structure in other copolyester systems showed similar enhanced elasticity and ductility. Wu et al.[37] synthesize a polyolefin-like copolymer from renewable 1,12-dodecanedioic acid (DDCA) and diol. By modulating the chain segment length, the copolymer's toughness is significantly enhanced, achieving a high-performance, sustainable material. The resulting biobased elastomer demonstrates excellent biocompatibility and an elastic recovery rate of 69.0% (T60-DA30). Likewise, Zuo et al.[38] successfully synthesized a fully biobased copolyester exhibiting superior mechanical and gas barrier properties through the incorporation of long-chain dicarboxylic acids (DDCA) into thiophene-containing polyesters. The findings demonstrate that the addition of a small proportion of DDCA effectively modulates the crystalline morphology of the copolyester. This modification transforms the inherently brittle PPThF homopolyester into a ductile material (PPDThF-10 copolyester) while concurrently preserving its high modulus, strength, and excellent barrier characteristics. The resultant PPDThF-10 copolyester exhibits performance metrics comparable to those of conventional packaging polymers such as polyethylene (PE) and polypropylene (PP). Consequently, this study successfully resolves the critical performance-sustainability trade-off by achieving a material with high toughness, superior barrier properties, and high optical transparency. Jia et al.[42] synthesized a series of fully biobased copolyesters derived from biosourced monomers DDCA, FDCA, and EG via a two-step melt polycondensation process, spanning the entire composition range. With increasing DDCA unit content, the morphology of the copolyesters transitioned progressively from amorphous elastomers to semicrystalline thermoplastics. Notably, the materials demonstrated elastic characteristics comparable to those of commercial TPE. Chen et al.[55] modified poly(butylene laurate) by incorporating aromatic and aliphatic ring structures into the polymer backbone. Their study demonstrated that introducing 70 mol % aromatic rings significantly suppressed the biodegradability of the resulting copolyesters. Conversely, incorporating the same proportion of aliphatic rings substantially enhanced the degradation rate. Notably, the aliphatic-modified copolyester exhibits biodegradability while simultaneously offering superior and tunable material properties across a broader range.

Based on the design of structurally similar biobased polyester materials and the study of structure−property relationships, it can be seen that the mechanical properties of the materials in this work improve significantly with increasing content of long-chain units (DDCA%). In this study, copolymer modification was performed on highly crystalline and heat-resistant biobased polyester (PCF) to simultaneously retain its excellent thermal properties and impart elasticity, thereby enhancing its applicability for potential applications. Performance comparisons demonstrate that polyethylene-like long-chain units exhibit recovery characteristics comparable to those of polyether soft-segment polyester elastomers.

3.4. Thermo-Mechanical Performance and Morphology Evolution. The thermo-mechanical behavior of the PCDF copolyesters with varying molar compositions was investigated using dynamic mechanical analysis (DMA)

https://doi.org/10.1021/acs.macromol.5c01114
Macromolecules 2025, 58, 8833−8844

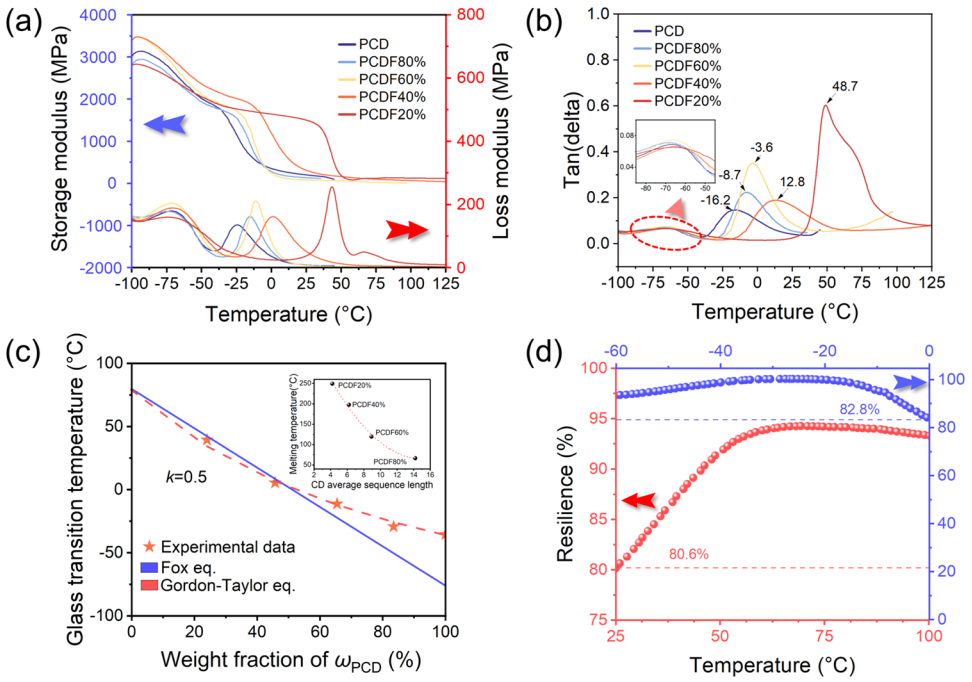

Figure 4. (a) Dynamic mechanical analysis of PCDF copolyesters and (b) tan delta as a function of temperature of PCDF copolyesters. (c) Composition dependence of T_g for PCDF copolyesters and relationships between T_m of PCDF copolyesters and correlations with CD average sequence length. (d) Resilience as a function of high-temperature and low-temperature, respectively.

measurements in the tensile mode. Figure 4a presents the temperature dependence of the storage modulus (E') for the copolyester films, indicating the mechanical response across a broad temperature range within the linear viscoelastic region. Only one transition was observed within the experimental temperature range, specifically, the glass transition. The T_g values obtained were comparable to those measured by DSC. Figure 4b illustrates the loss tangent (tan δ) as a function of temperature, where tan δ serves as the damping factor measured through DMA. The storage modulus was found to decrease with an increase in PCD, which can be attributed to the enhanced flexibility of the polyesters. The α relaxation peak of the homopolyester PCD is significantly lower than those of the PCDF copolyesters, primarily due to the reversible characteristics that allow the elastomers to exhibit sufficient softness for high flexibility while maintaining adequate stiffness for handling. As the φ_{CD} increases, the peak height of tan δ decreases, indicating a reduction in the damping effect, which suggests improved compatibility between the two segments. This also implies that the thermodynamic compatibility between the two chain segments progressively transitions from miscibility to compatibility. As illustrated in Figure 4c, the composition-dependent T_g of the PCDF random copolyesters aligns well with the established Gordon−Taylor eq (eq 5), with the adjustable parameter k set to 0.5.

$$T_g = T_{g,PCF}\cdot\omega_{PCF} + T_{g,PCD}\cdot\omega_{PCD} \quad (3)$$

$$T_g = \frac{T_{g,PCF}\cdot\omega_{PCF} + kT_{g,PCD}\cdot\omega_{PCD}}{\omega_{PCF} + k\omega_{PCD}} \quad (4)$$

The excellent resilience of PCDF60% was further investigated across wider temperature and frequency ranges according to the following equation

$$\text{resilience}\ (\%) = e^{-1/2\pi\tan(\delta)} \times 100 \quad (5)$$

where the tan δ is the damping factor measured through DMA. Figure 4d indicates that PCDF60% maintains a high resilience, exceeding 80.6 and 82.8% across broad temperature ranges of 25−100 °C and −60−0 °C, respectively. This demonstrates significant independence from temperature.

In comparison with the Fox equation calculations, the disparity between the theoretical T_g obtained from the linear fit and the measured T_g is substantial. This suggests that the composition of the aggregated state structure fundamentally changes with increasing DDCA content, resulting in a transformation toward a more orthorhombic crystalline structure akin to that of PE. When the storage modulus significantly exceeds the loss modulus, the material predominantly exhibits elastic deformation. The superior performance of the material can be attributed to two key features: (1) highly entangled polymer chain in the amorphous region and (2) reversible properties stemming from nonplanar rings when subjected to external deformation. Furthermore, entanglements function as slip-links, facilitating the transmission of tensile stress along the chain and to adjacent chains by adjustment of their positions during elongation of the elastomer.

To effectively combine the advantages of these two materials, it is crucial to establish a connection between the PCD chain segments, which partially generates a PE-like structure. In elastic polymer systems, morphological evolution plays a vital role in regulating and improving the mechanical properties. SAXS patterns of the semicrystalline copolyesters reveal phase ordering consistent with the crystallinity. The long period distance (L) can be calculated from the 2θ values at specific SAXS intensities using Bragg's equation ($L = 2\pi/q_{max}$). Additionally, the lamellar thickness (l_c) and average amorphous layer thickness (l_a) in the lamellar stacks can be derived from WAXS and SAXS data using eq (S6−S8), assuming that the amorphous region is located solely within

https://doi.org/10.1021/acs.macromol.5c01114
Macromolecules 2025, 58, 8833−8844

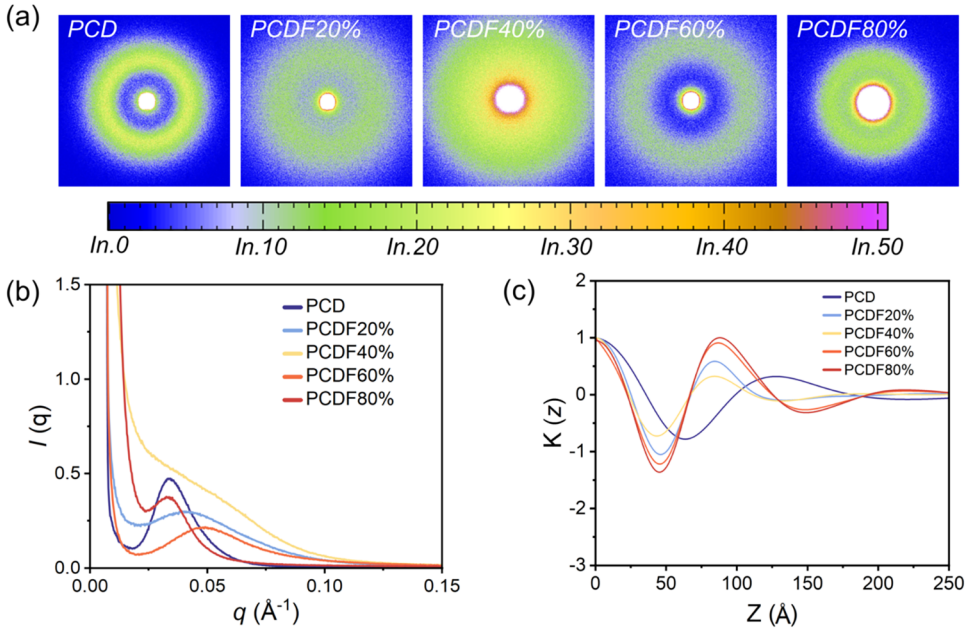

Figure 5. Selected (a) 2D and (b) 1D SAXS patterns and (c) normalized 1D correlation function curves of the SAXS profile for PCDF copolyesters.

the lamellar stacks. SAXS analyses were conducted to investigate the excellent resilience and morphological evolution of the PCDF, as illustrated in Figures 5a and S4,S5 (Supporting Information). Simulations of the particle size distribution for PCDFs with a polyethylene-like structure confirmed that the periodicity of their microscopic structure exhibits identical strong dependencies on both polydispersity and interaction strength, as observed in polyolefin elastomers (see Figure S5). Numerous morphological details of PCDF copolyesters, beyond those inferred from the Lorentz-corrected SAXS diffractograms, can be obtained through analysis of the correlation function, which represents the Fourier transform of the intensity function. Given the semicrystalline structure of copolyesters, it is essential to examine the variations in electron density along the longitudinal direction (Figure 5c). The average values of the long period (L), l_c, and l_a were calculated by a one-dimensional correlation function, $K(z)$. Consequently, only the corresponding 1D correlation function is relevant, which can be expressed as follows

$$K(z) = \frac{\int_0^\infty qI^2(q)\cos(qz)\mathrm{d}q}{\int_0^\infty I(q)q^2\mathrm{d}q} \tag{6}$$

Thermodynamically, the radius distribution (i.e., size distribution) of PCDF copolyesters particles follows the Schultz-Zimm function,[33] as evidenced by the obtained distribution parameters. The scattering profile has been attempted to be analyzed in a qualitative manner by using the indirect Fourier transformation (IFT) analysis, which is a model-independent scattering analysis method.[33,S6] Figure 5 and eq S6−S8 displays the 1D SAXS profiles and 2D patterns for all samples. In order to elucidate the relationship between the sequence alignment structure and particle distribution, we combined experimental characterization with molecular dynamics simulations to simulate the particle distribution of PCDF60%. By simulation of the particle distribution of PCDF60% copolyester, it can be seen that the system has a very narrow single-peak size distribution and is spherical. In addition, such a tight density distribution facilitates the entanglement to act as a slippery chain, and when the elastomer is stretched, the tension is transferred along the chain to other chains by adjustment of the position of the chain. Like TPEs,[17,19,25] as shown in Figure S4, PCDF40% also exhibits a wide distribution of amorphous regions; however, its layer thickness distribution is narrower. This narrower distribution explains the disappearance of yield behavior and the emergence of rubber-like behavior similar to elastomers.

4. CONCLUSIONS

In summary, a series of biobased high molecular weight furan copolyesters (PCDF) were synthesized through a two-stage melt polycondensation method, utilizing CHDM, DDCA with a long-chain structure, and FDCA as the raw materials. The resulting copolyesters exhibited different crystalline and mechanical properties based on the ratio of aliphatic DDCA to aromatic FDCA used in the copolymerization process. The PCDF copolyesters displayed a semicrystalline nature, characterized by distinct heat of fusion absorption and low-intensity crystalline peaks. Notably, at a 60% ratio of φ_{CD}, the copolyester segregated into two predominant crystalline forms. The polyethylene-like structure formed from the polymerization of the long-chain diacid with nonplanar diols contributed to the enhanced toughness of the material, demonstrating the characteristics of stress-hardened thermoplastic elastomers. As the φ_{CD} ratio increased, PCDF60% achieved optimal elastic recovery (η_{r1} = 64.0%) and excellent rigidity (E_t = 52 MPa). These findings indicate that thermoplastic polyester elastomers devoid of polyether soft segments were successfully developed, and this design strategy provides a viable solution and theoretical guidance for the advancement of green high-performance elastomers.

https://doi.org/10.1021/acs.macromol.5c01114
Macromolecules 2025, 58, 8833−8844

■ ASSOCIATED CONTENT

Supporting Information

The Supporting Information is available free of charge at https://pubs.acs.org/doi/10.1021/acs.macromol.5c01114.

Sample treatment; GPC profiles; cyclic tensile testing strain−stress curves; reaction conditions; thermal properties (TGA and DTG curves); aggregation structure (SAXS profile), and elastic and tensile properties (PDF)

■ AUTHOR INFORMATION

Corresponding Authors

Fei Liu − *Key Laboratory of Biobased Polymeric Materials of Zhejiang Province, Ningbo Institute of Materials Technology and Engineering, Chinese Academy of Sciences, Ningbo, Zhejiang 315201, China;* orcid.org/0000-0002-7848-5226; Email: liufei@nimte.ac.cn

Jinggang Wang − *Key Laboratory of Biobased Polymeric Materials of Zhejiang Province, Ningbo Institute of Materials Technology and Engineering, Chinese Academy of Sciences, Ningbo, Zhejiang 315201, China;* orcid.org/0000-0002-4652-0170; Email: wangjg@nimte.ac.cn

Authors

Yajin Fang − *Key Laboratory of Biobased Polymeric Materials of Zhejiang Province, Ningbo Institute of Materials Technology and Engineering, Chinese Academy of Sciences, Ningbo, Zhejiang 315201, China*

Tao Yang − *Key Laboratory of Biobased Polymeric Materials of Zhejiang Province, Ningbo Institute of Materials Technology and Engineering, Chinese Academy of Sciences, Ningbo, Zhejiang 315201, China*

Jin Zhu − *Key Laboratory of Biobased Polymeric Materials of Zhejiang Province, Ningbo Institute of Materials Technology and Engineering, Chinese Academy of Sciences, Ningbo, Zhejiang 315201, China*

Complete contact information is available at: https://pubs.acs.org/10.1021/acs.macromol.5c01114

Notes

The authors declare no competing financial interest.

■ ACKNOWLEDGMENTS

We are grateful for the financial support by the National Key R&D Program of China (2021YFB3700300), Ningbo Scientific Innovation Yongjiang 2035 Programs (2024Z100), Quzhou Joint Fund of the Zhejiang Provincial Natural Science Foundation of China (LQZSZ25E030003), and Zhejiang Provincial Key Scientific Research Programs (2023C01101).

■ REFERENCES

(1) Chen, S.; Wang, Y.; Yang, L.; Chu, C.; Cao, S.; Wang, Z.; Xue, J.; You, Z. Biodegradable Elastomers for Biomedical Applications. *Prog. Polym. Sci.* **2023**, *147*, No. 101763.

(2) Steube, M.; Johann, T.; Barent, R. D.; Müller, A. H. E.; Frey, H. Rational Design of Tapered Multiblock Copolymers for Thermoplastic Elastomers. *Prog. Polym. Sci.* **2022**, *124*, No. 101488.

(3) Aarsen, C. V.; Liguori, A.; Mattsson, R.; Sipponen, M. H.; Hakkarainen, M. Designed to Degrade: Tailoring Polyesters for Circularity. *Chem. Rev.* **2024**, *124* (13), 8473−8515.

(4) Ye, H.; Zhang, K.; Kai, D.; Li, Z.; Loh, X. J. Polyester Elastomers for Soft Tissue Engineering. *Chem. Soc. Rev.* **2018**, *47* (12), 4545−4580.

(5) Sun, D.; Mo, J.; Liu, W.; Yan, N.; Qiu, X. Ultra-Strong and Tough Bio-Based Polyester Elastomer with Excellent Photothermal Shape Memory Effect and Degradation Performance. *Adv. Funct. Mater.* **2024**, *34*, No. 2403333.

(6) Huyer, L. D.; Bannerman, A. D.; Wang, Y.; Savoji, H.; Knee-Walden, E. J.; Brissenden, A.; Yee, B.; Shoaib, M.; Bobicki, E.; Amsden, B. G.; Radisic, M. One-Pot Synthesis of Unsaturated Polyester Bioelastomer with Controllable Material Curing for Microscale Designs. *Adv. Healthcare Mater.* **2019**, *8* (16), No. 1900245.

(7) Banerjee, A.; Dick, G. R.; Yoshino, T.; Kanan, M. W. Carbon Dioxide Utilization via Carbonate-Promoted C−H Carboxylation. *Nature* **2016**, *531* (7593), 215−219.

(8) Horejs, C. Solutions to Plastic Pollution. *Nat. Rev. Mater.* **2020**, *5* (9), 641.

(9) Abel, B. A.; Snyder, R. L.; Coates, G. W. Chemically Recyclable Thermoplastics from Reversible-Deactivation Polymerization of Cyclic Acetals. *Science* **2021**, *373*, 783−789.

(10) Zhao, Y.; Cai, M.; Xian, J.; Sun, Y.; Li, G. Recent Advances in the Electrocatalytic Synthesis of 2,5-Furandicarboxylic Acid from 5-(Hydroxymethyl)Furfural. *J. Mater. Chem. A* **2021**, *9* (36), 20164−20183.

(11) Fei, X.; Wang, J.; Zhu, J.; Wang, X.; Liu, X. Biobased Poly(Ethylene 2,5-Furancoate): No Longer an Alternative, but an Irreplaceable Polyester in the Polymer Industry. *ACS Sustainable Chem. Eng.* **2020**, *8* (23), 8471−8485.

(12) Sun, L.; Wang, J.; Mahmud, S.; Jiang, Y.; Zhu, J.; Liu, X. New Insight into the Mechanism for the Excellent Gas Properties of Poly(Ethylene 2,5-Furandicarboxylate) (PEF): Role of Furan Ring's Polarity. *Eur. Polym. J.* **2019**, *118*, 642−650.

(13) Burgess, S. K.; Leisen, J. E.; Kraftschik, B. E.; Mubarak, C. R.; Kriegel, R. M.; Koros, W. J. Chain Mobility, Thermal, and Mechanical Properties of Poly(Ethylene Furanoate) Compared to Poly(Ethylene Terephthalate). *Macromolecules* **2014**, *47* (4), 1383−1391.

(14) Hu, H.; Zhang, R.; Sousa, A.; Yu, L.; Ying, W. B.; Wang, J.; Zhu, J. Bio-Based Poly(Butylene 2,5-Furandicarboxylate)-b-Poly-(Ethylene Glycol) Copolymers with Adjustable Degradation Rate and Mechanical Properties: Synthesis and Characterization. *Eur. Polym. J.* **2018**, *106*, 42−52.

(15) Xie, H.; Wu, L.; Li, B.-G.; Dubois, P. Poly(Ethylene 2,5-Furandicarboxylate-Mb-Poly(Tetramethylene Glycol)) Multiblock Copolymers: From High Tough Thermoplastics to Elastomers. *Polymer* **2018**, *155*, 89−98.

(16) Zhou, W.; Zhang, Y.; Xu, Y.; Wang, P.; Gao, L.; Zhang, W.; Ji, J. Synthesis and Characterization of Bio-Based Poly(Butylene Furandicarboxylate)-b-Poly(Tetramethylene Glycol) Copolymers. *Polym. Degrad. Stab.* **2014**, *109*, 21−26.

(17) Yang, T.; Liu, F.; Gao, R.; Li, J.; Wang, J.; Zhu, J. Rational Design for the Development of Thermoplastic Poly(Ether-Ester) Elastomers from Bio-Based 2,5-Furandicarboxylic Acid with High Elasticity. *Eur. Polym. J.* **2023**, *198*, No. 112385.

(18) Yang, T.; Liu, F.; Gao, R.; Zhang, X.; Li, J.; Wang, J.; Zhu, J. Fabrication of Thermoplastic Poly(Ether-Ester) Elastomers with High Melting Temperature and Elasticity from Bio-Based 2,5-Furandicarboxylic Acid. *ACS Sustainable Resour. Manage.* **2024**, *1* (7), 1520−1533.

(19) Gao, R.; Wang, J.; Liu, F.; Dai, H.; Zhang, X.; Wang, X.; Li, Y.; Zhu, J. Synthesis of Bio-Based Poly(Ester-Ether) Elastomers from 2,5-Furandicarboxylic Acid (FDCA) with Excellent Thermo-Mechanical Properties. *Polym. Degrad. Stab.* **2023**, *210*, No. 110292.

(20) Wang, J.; Zhang, X.; Fei, X.; Gao, R.; Liu, F.; Fan, L.; Zhu, J.; Liu, X. Synthesis of High Thermal-Resistant Poly(Ester-Ether) Elastomers from Bio-Based 2,5-Furandicarboxylic Acid. *ACS Sustainable Chem. Eng.* **2022**, *10* (41), 13595−13606.

(21) Chi, D.; Liu, F.; Na, H.; Chen, J.; Hao, C.; Zhu, J. Poly(Neopentyl Glycol 2,5-Furandicarboxylate): A Promising Hard Segment for the Development of Bio-Based Thermoplastic Poly-(Ether-Ester) Elastomer with High Performance. *ACS Sustainable Chem. Eng.* **2018**, *6* (8), 9893−9902.

(22) Mondschein, R. J.; Dennis, J. M.; Liu, H.; Ramakrishnan, R. K.; Sirrine, J. M.; Weiseman, T.; Colby, R. H.; Nazarenko, S.; Turner, S. R.; Long, T. E. Influence of Bibenzoate Regioisomers on Cyclohexanedimethanol-Based (Co)Polyester Structure−Property Relationships. *Macromolecules* **2019**, *52* (3), 835−843.
(23) Hahm, S.; Kim, J.-S.; Yun, H.; Park, J. H.; Letteri, R. A.; Kim, B. J. Bench-Scale Synthesis and Characterization of Biodegradable Aliphatic−Aromatic Random Copolymers with 1,4-Cyclohexanedimethanol Units Toward Sustainable Packaging Applications. *ACS Sustainable Chem. Eng.* **2019**, *7* (5), 4734−4743.
(24) Jin, C.; Tian, W.; Tu, Z.; Wei, Z. Kilogram-Scale Production of Sustainable PCF Copolyesters Based on Novel Cyclic Diol THFDM Derived from 5-Hydroxymethylfurfural: Trade-Off between the THFDM Structure and Various Properties of Copolyesters. *ACS Sustainable Chem. Eng.* **2021**, *9* (39), 13287−13302.
(25) Yang, T.; Zuo, J.; Liu, F.; Liu, C.; Chen, C.; Jiang, X.; Liu, K.; Yu, S.; Wang, J.; Zhu, J. Bio-Based Thermoplastic Poly(Ether-Ester) Elastomers from 2,5-Thiophenedicarboxylic Acid with High Stiffness and Elasticity. *Chem. Eng. J.* **2025**, *510*, No. 161856.
(26) Lim, A.-Y.; Park, S. B.; Choi, Y.; Oh, D. X.; Park, J.; Jeon, H.; Koo, J. M. Extending the High-Performing Boundaries of a Fully Bio-Based Thermal Shrinkage Film Targeted for Food Packaging Applications. *Green Chem.* **2023**, *25*, 9711−9719, DOI: 10.1039/D3GC02193A.
(27) Liu, F.; Zhang, J.; Wang, J.; Liu, X.; Zhang, R.; Hu, G.; Na, H.; Zhu, J. Soft Segment Free Thermoplastic Polyester Elastomers with High Performance. *J. Mater. Chem. A* **2015**, *3* (26), 13637−13641.
(28) Neng, W.-B.; Xie, W.-G.; Lu, B.; Zhen, Z.-C.; Zhao, J.-L.; Wang, G.-X.; Ji, J.-H. Biodegradable Thermoplastic Copolyester Elastomers: Methyl Branched PBA $_m$ T. *e-Polymers* **2021**, *21* (1), 336−345.
(29) Sahu, P.; Sharma, L.; Dawsey, T.; Gupta, R. K. Fully Biobased High-Molecular-Weight Polyester with Impressive Elasticity, Thermo-Mechanical Properties, and Enzymatic Biodegradability: Replacing Terephthalate. *Macromolecules* **2024**, *57* (19), 9302−9314.
(30) Eck, M.; Mecking, S. Closed-Loop Recyclable and Non-persistent Polyethylene-like Polyesters. *Acc. Chem. Res.* **2024**, *57* (6), 971−980.
(31) Häußler, M.; Eck, M.; Rothauer, D.; Mecking, S. Closed-Loop Recycling of Polyethylene-like Materials. *Nature* **2021**, *590* (7846), 423−427.
(32) Nelson, T. F.; Rothauer, D.; Sander, M.; Mecking, S. Degradable and Recyclable Polyesters from Multiple Chain Length Bio- and Waste-Sourceable Monomers. *Angew. Chem., Int. Ed.* **2023**, *62* (43), No. e202310729.
(33) Glatter, O. A New Method for the Evaluation of Small-Angle Scattering Data. *J. Appl. Crystallogr.* **1977**, *10* (5), 415−421.
(34) Stępień, K.; Miles, C.; McClain, A.; Wiśniewska, E.; Sobolewski, P.; Kohn, J.; Puskas, J.; Wagner, H. D.; El Fray, M. Biocopolyesters of Poly(Butylene Succinate) Containing Long-Chain Biobased Glycol Synthesized with Heterogeneous Titanium Dioxide Catalyst. *ACS Sustainable Chem. Eng.* **2019**, *7* (12), 10623−10632.
(35) Gu, S.; Zhu, F.; Zhang, L.; Wen, J. Mid−Long Chain Dicarboxylic Acid Production via Systems Metabolic Engineering: Progress and Prospects. *J. Agric. Food Chem.* **2024**, *72* (11), 5555−5573.
(36) Zhou, C.; Wei, Z.; Yu, Y.; Shao, S.; Leng, X.; Wang, Y.; Li, Y. Biobased Long-Chain Aliphatic Polyesters of 1,12-Dodecanedioic Acid with a Variety of Diols: Odd-Even Effect and Mechanical Properties. *Mater. Today Commun.* **2019**, *19*, 450−458.
(37) Wu, X.; Yang, T.; Jiang, X.; Su, W.; Liu, F.; Wang, J.; Zhu, J. New Thermoplastic Poly(Ester−Ether) Elastomers with Enhanced Mechanical Properties Derived from Long-Chain Dicarboxylic Acid for Medical Device Applications. *J. Mater. Chem. B* **2025**, *13* (5), 1731−1743.
(38) Zuo, J.; Yang, T.; Lin, C.; Deng, H.; Gu, S.; Liu, F.; Shen, Z.; Zhu, J.; Wang, J. Fully Biobased Copolyesters with High Gas Barrier and Enhanced Mechanical Properties Derived from 2,5-Thiophenedicarboxylic Acid and Long-Chain Dicarboxylic Acid. *ACS Sustainable Chem. Eng.* **2025**, *13* (4), 1775−1787.
(39) Strobl, G. Crystallization and Melting of Bulk Polymers: New Observations, Conclusions and a Thermodynamic Scheme. *Prog. Polym. Sci.* **2006**, *31* (4), 398−442.
(40) Schulz, M.; Schäfer, M.; Saalwächter, K.; Thurn-Albrecht, T. Competition between Crystal Growth and Intracrystalline Chain Diffusion Determines the Lamellar Thickness in Semicrystalline Polymers. *Nat. Commun.* **2022**, *13* (1), No. 119.
(41) Strobl, G. R.; Schneider, M. Direct Evaluation of the Electron Density Correlation Function of Partially Crystalline Polymers. *J. Polym. Sci., Polym. Phys. Ed.* **1980**, *18* (6), 1343−1359.
(42) Jia, Z.; Wang, J.; Sun, L.; Zhu, J.; Liu, X. Fully Bio-based Polyesters Derived from 2,5-furandicarboxylic Acid (2,5-FDCA) and Dodecanedioic Acid (DDCA): From Semicrystalline Thermoplastic to Amorphous Elastomer. *J. Appl. Polym. Sci.* **2018**, *135* (14), No. 46076.
(43) Hong, S.; Min, K.-D.; Nam, B.-U.; Park, O. O. High Molecular Weight Bio Furan-Based Co-Polyesters for Food Packaging Applications: Synthesis, Characterization and Solid-State Polymerization. *Green Chem.* **2016**, *18* (19), 5142−5150.
(44) Wang, J.; Liu, X.; Zhang, Y.; Liu, F.; Zhu, J. Modification of Poly(Ethylene 2,5-Furandicarboxylate) with 1,4-Cyclohexanedimethylene: Influence of Composition on Mechanical and Barrier Properties. *Polymer* **2016**, *103*, 1−8.
(45) Tian, S.; Shi, K.; Xu, J.; Guo, B. Synthesis and Structure−Property Relationships of Novel High Molecular Weight Fully Biobased 2,5-Thiophenedicarboxylic Acid-Based Polyesters. *Biomacromolecules* **2023**, *24*, No. acs.biomac.3c00001.
(46) Hu, H.; Zhang, R.; Ying, W. B.; Kong, Z.; Wang, K.; Wang, J.; Zhu, J. Biodegradable Elastomer from 2,5-Furandicarboxylic Acid and ε-Caprolactone: Effect of Crystallization on Elasticity. *ACS Sustainable Chem. Eng.* **2019**, *7* (21), 17778−17788.
(47) Matos, M.; Sousa, A. F.; Silvestre, A. J. D. Improving the Thermal Properties of Poly(2,5-furandicarboxylate)s Using Cyclohexylene Moieties: A Comparative Study. *Macromol. Chem. Phys.* **2017**, *218* (5), No. 1600492.
(48) Hu, H.; Zhang, R.; Wang, J.; Ying, W. B.; Zhu, J. Fully Bio-Based Poly(Propylene Succinate-Co-Propylene Furandicarboxylate) Copolyesters with Proper Mechanical, Degradation and Barrier Properties for Green Packaging Applications. *Eur. Polym. J.* **2018**, *102*, 101−110.
(49) Liu, L.; He, C.; Zhu, L.; Zhu, Z.; Xiao, K. Preparation of Degradable Modified Atmosphere Films by Blending Polybutylene Glycol 2,5-Furandicarboxylate - Polytetrahydrofurandiol Polyether Esters with Poly (Butyleneadipate-Co-Terephthalate) and Its Application in Strawberry Preservation. *Food Packag. Shelf Life* **2025**, *47*, No. 101446.
(50) Liu, F.; Qiu, J.; Wang, J.; Zhang, J.; Na, H.; Zhu, J. Role of Cis-1,4-Cyclohexanedicarboxylic Acid in the Regulation of the Structure and Properties of a Poly(Butylene Adipate-Co-Butylene 1,4-Cyclohexanedicarboxylate) Copolymer. *RSC Adv.* **2016**, *6* (70), 65889−65897.
(51) Liu, F.; Zhang, J.; Wang, J.; Na, H.; Zhu, J. Incorporation of 1,4-Cyclohexanedicarboxylic Acid into Poly(Butylene Terephthalate)-b-Poly(Tetramethylene Glycol) to Alter Thermal Properties without Compromising Tensile and Elastic Properties. *RSC Adv.* **2015**, *5* (114), 94091−94098.
(52) Chen, J.; Huang, W.; Xu, Q.; Tu, Y.; Zhu, X.; Chen, E. PBT-b-PEO-b-PBT Triblock Copolymers: Synthesis, Characterization and Double-Crystalline Properties. *Polymer* **2013**, *54* (25), 6725−6731.
(53) Szymczyk, A. Structure and Properties of New Polyester Elastomers Composed of Poly(Trimethylene Terephthalate) and Poly(Ethylene Oxide). *Eur. Polym. J.* **2009**, *45* (9), 2653−2664.
(54) Szymczyk, A.; Nastalczyk, J.; Sablong, Rj.; Roslaniec, Z. The Influence of Soft Segment Length on Structure and Properties of Poly(Trimethylene Terephthalate)-Block-Poly(Tetramethylene Oxide) Segmented Random Copolymers. *Polym. Adv. Technol.* **2011**, *22* (1), 72−83.

https://doi.org/10.1021/acs.macromol.5c01114
Macromolecules 2025, 58, 8833−8844

(55) Chen, M.; Saada, N. A. H.; Liu, F.; Na, H.; Zhu, J. Synthesis of Copolyesters with Bio-Based Lauric Diacid: Structure and Physico-Mechanical Studies. *RSC Adv.* **2017**, *7* (87), 55418−55426.
(56) Arbe, A.; Rubio-Cervilla, J.; Alegría, A.; Moreno, A. J.; Pomposo, J. A.; Robles-Hernández, B.; Malo De Molina, P.; Fouquet, P.; Juranyi, F.; Colmenero, J. Mesoscale Dynamics in Melts of Single-Chain Polymeric Nanoparticles. *Macromolecules* **2019**, *52* (18), 6935−6942.

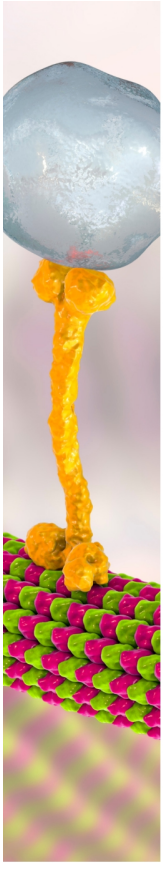
CAS BIOFINDER DISCOVERY PLATFORM™
BRIDGE BIOLOGY AND CHEMISTRY FOR FASTER ANSWERS
Analyze target relationships, compound effects, and disease pathways
Explore the platform
CAS
A division of the American Chemical Society

https://doi.org/10.1021/acs.macromol.5c01114
Macromolecules 2025, 58, 8833−8844